Electronic Supplementary Material (ESI) for Journal of Materials Chemistry C.

Supplementary Information

Enhancing the Optoelectronic Properties of Solution-Processed $AgInSe_2$ Thin Films for Application in Photovoltaics

Shubhanshu Agarwal[a], Kyle Weidemann[a], David Rokke[a], Kiruba Catherine Vincent[a], Dmitry Zemlyanov[b], and Rakesh Agrawal[a,*]

[a.]Davidson School of Chemical Engineering, Purdue University, West Lafayette, Indiana 47907, United States

[b.]Birck Nanotechnology Center, Purdue University, West Lafayette, Indiana 47907, United States

*Rakesh Agrawal – Davidson School of Chemical Engineering, Purdue University, West Lafayette, Indiana 47907, United States

Email: agrawalr@purdue.edu

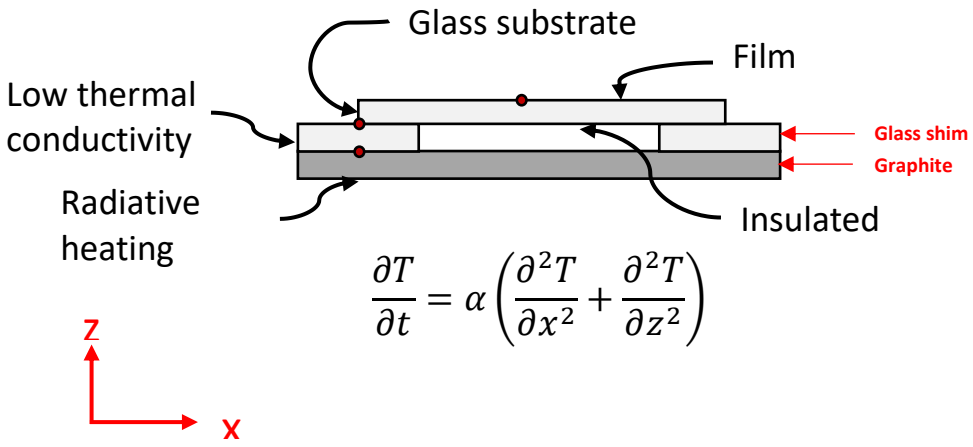

Figure S1. Schematic of the configuration modeled for the heat transfer calculations with the boundary conditions used (red dots indicate the points at which temperatures are plotted in Figure S2).

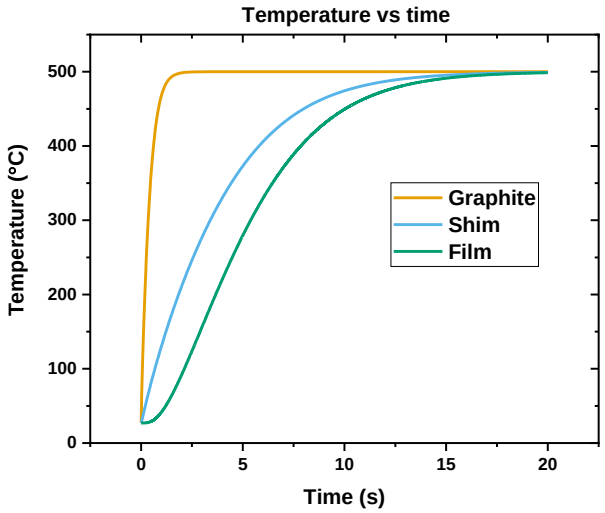

Figure S2. Temperature variation at the 3 points indicated in Figure S1 with time upon exposure to the surrounding maintained at 500 ^{o}C.

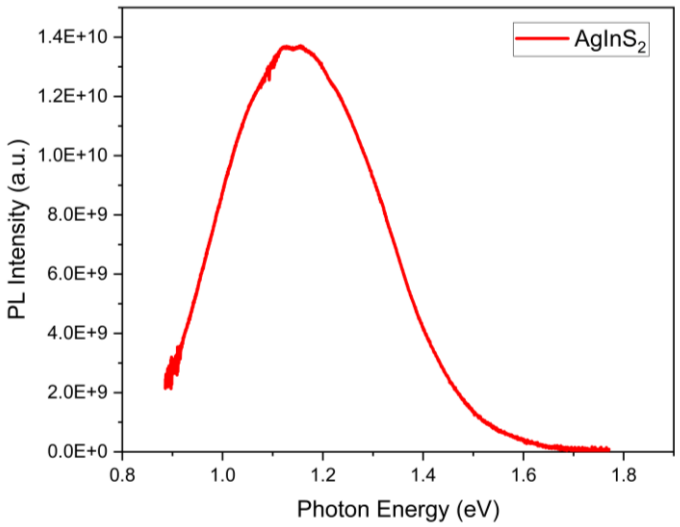

Figure S3. Photoluminescence plot of as-coated $AgInS_2$ film. The peak position at around 1.18 eV may correspond to some Ag_2S impurity.

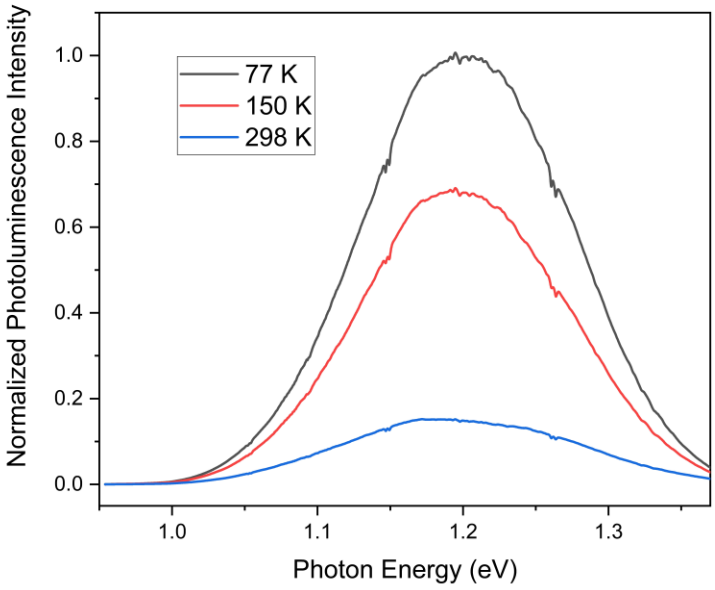

Figure S4. Variable temperature PL for the as-coated $AgInS_2$ film shows that the midgap peak PL intensity increased at low temperatures with a blue shift.

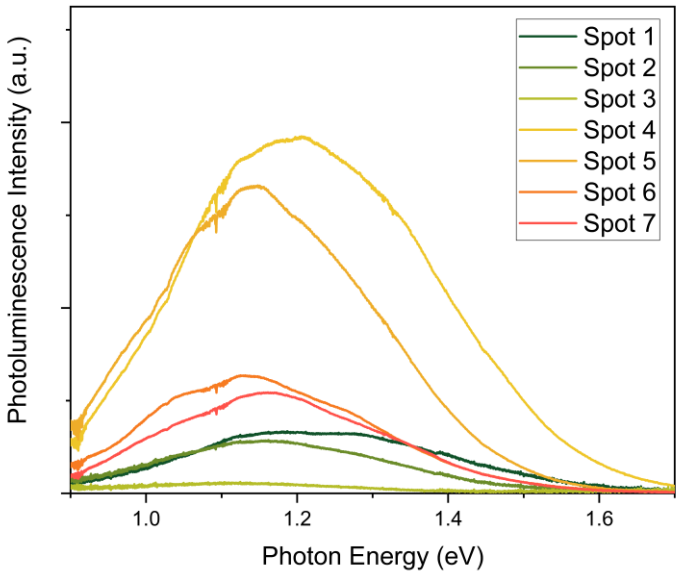

Figure S5. The midgap PL peak for the $AgInS_2$ film varied from spot to spot between 1.17 eV to 1.25 eV.

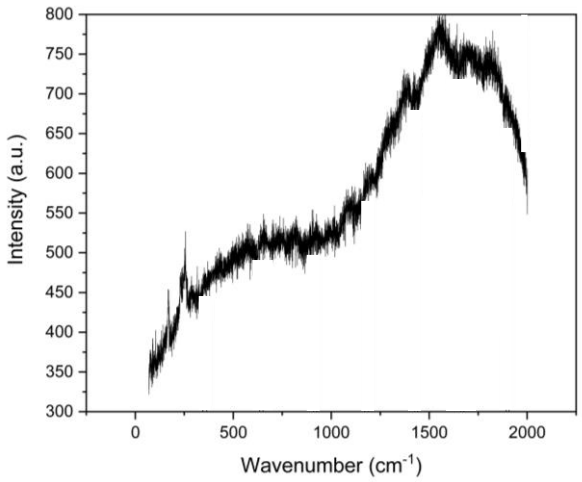

Figure S6. Raman spectrum shows the presence of residual amorphous carbon in the $AgInSe_2$ film after regular selenization of the Stoichiometric $AgInSe_2$ film prepared from DMF-TU-Chlorides ink.

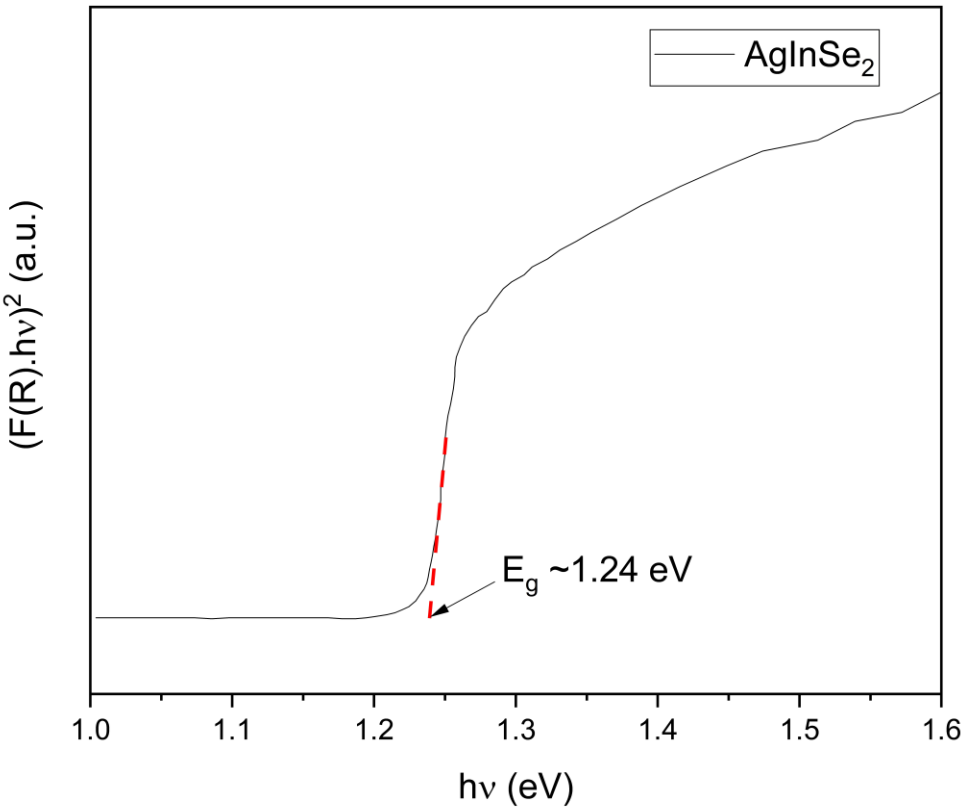

Figure S7. Bandgap of $AgInSe_2$ film obtained from the Kubelka-Munk transformation on diffuse reflectance spectra.

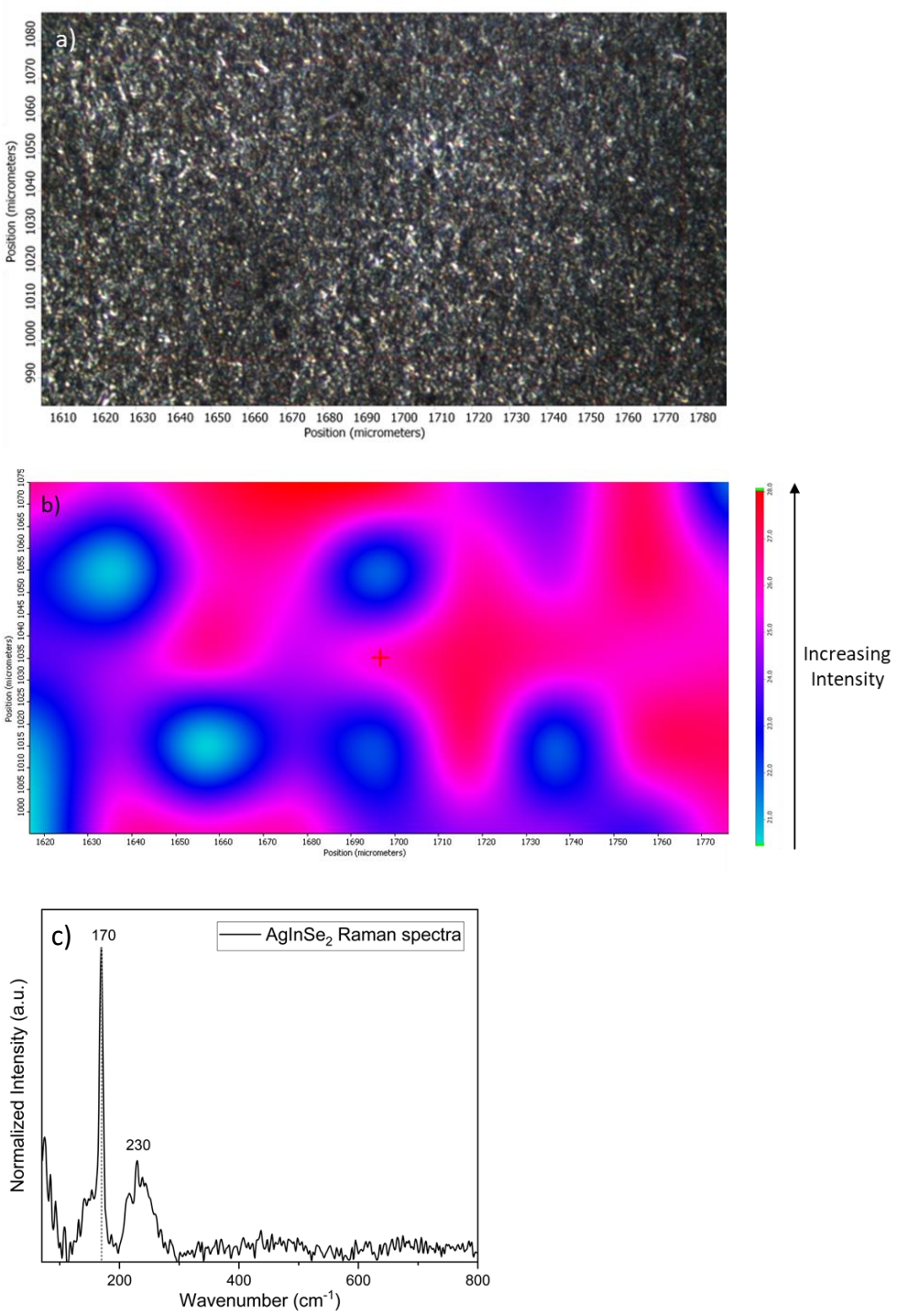

Figure S8. Raman mapping of the $AgInSe_2$ film selenized on shims at 515 ^{o}C, a) Optical Image of the screened portion of $AgInSe_2$ film, b) Intensity map of 170 cm^{-1} peak, and c) Raman spectrum.

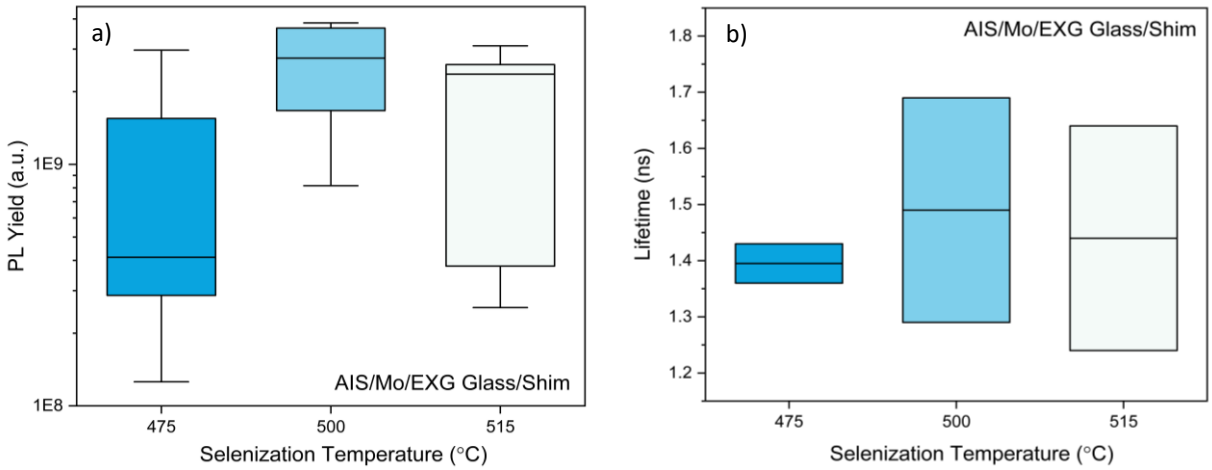

Figure S9. a) PL yield variation, b) Carrier lifetime variation with selenization temperature for the $AgInSe_2$ films selenized on shims with Molybdenum back contact.

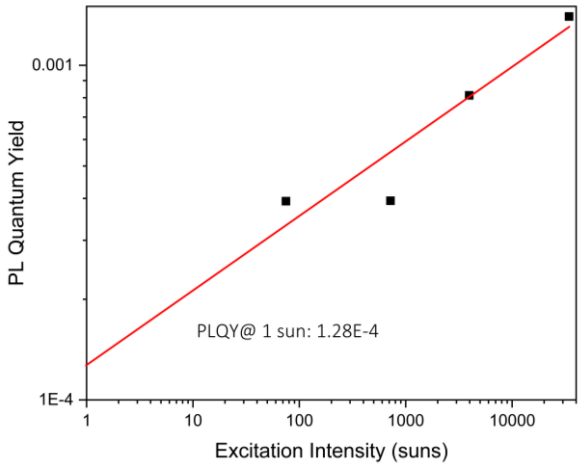

Figure S10. Plot showing the variation of the PLQY at different excitation intensities for the $AgInSe_2$ film on alumina coated EXG glass selenized at 515 ^{o}C on shims. The fitted curve was extrapolated to one-sun to estimate the PLQY at one-sun.

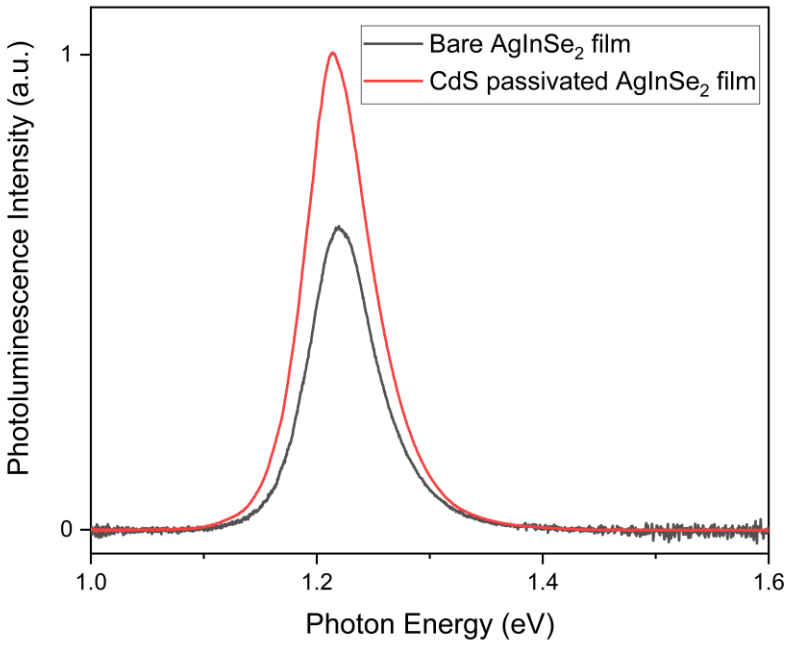

Figure S11. Comparison of the PL peak intensities for the $AgInSe_2$ films selenized with and without CdS passivation.

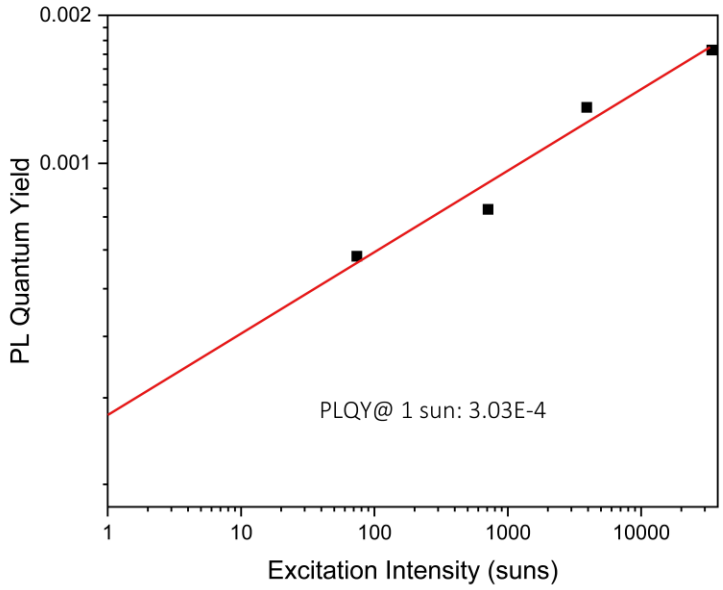

Figure S12. Plot showing the variation of the PLQY at different excitation intensities for the $AgInSe_2$ film passivated with CdS, deposited on alumina coated EXG glass and selenized at 515 ^{o}C on shims. The fitted curve was extrapolated to one-sun to estimate the PLQY at one-sun.

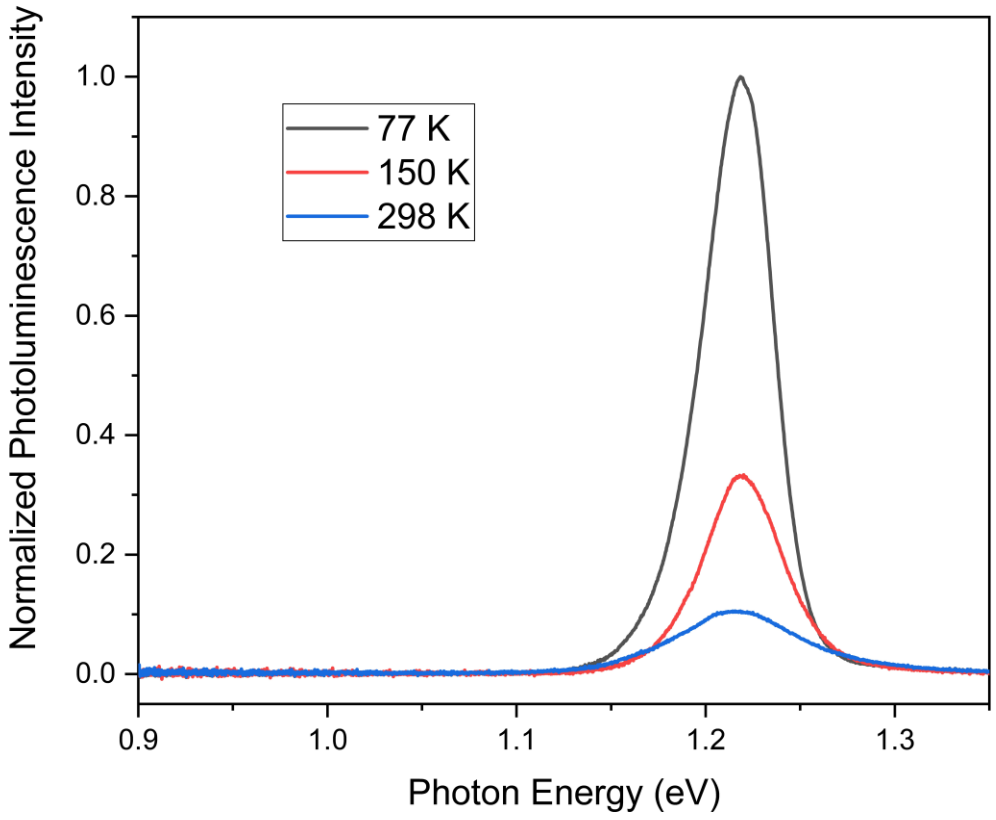

Figure S13. Variable temperature PL for the $AgInSe_2$ film selenized on shims shows that the band-to-band PL peak intensity increased at low temperatures.

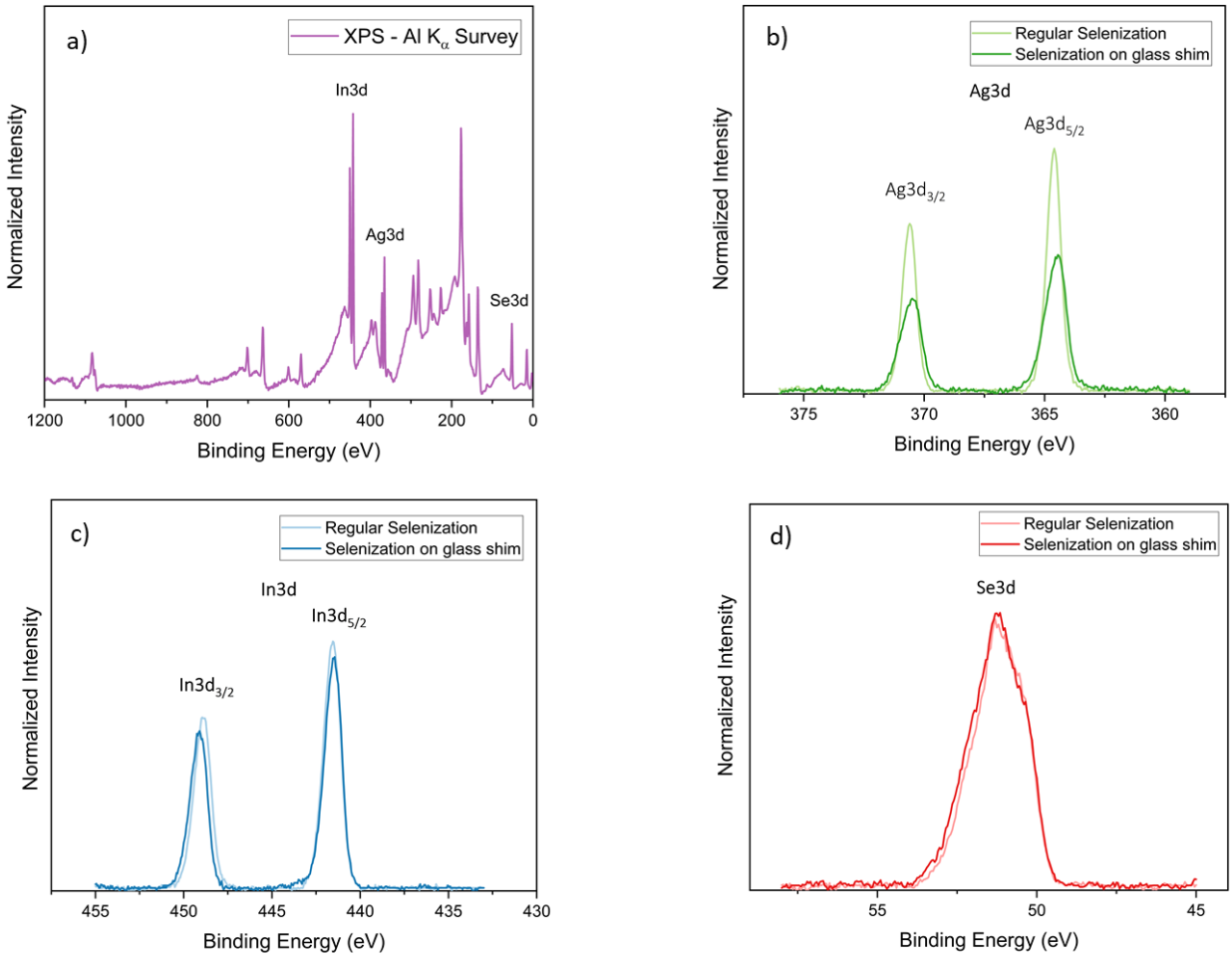

Figure S14. a) Full XPS spectra of $AgInSe_2$ film selenized on shims, b) Comparison of the Ag3d, c) Comparison of the In3d, and d) Comparison of the Se3d peaks for the $AgInSe_2$ films selenized at 515 ^{o}C without and with shims.

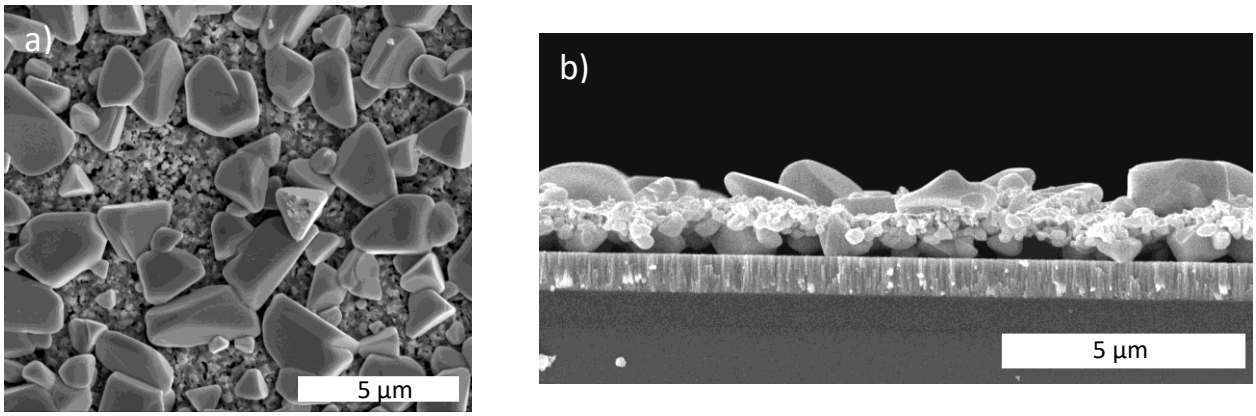

Figure S15. a) SEM top-view, b) SEM cross-sectional view of $AgInSe_2$ film selenized at 515 ^oC on shims with Mo back contact.

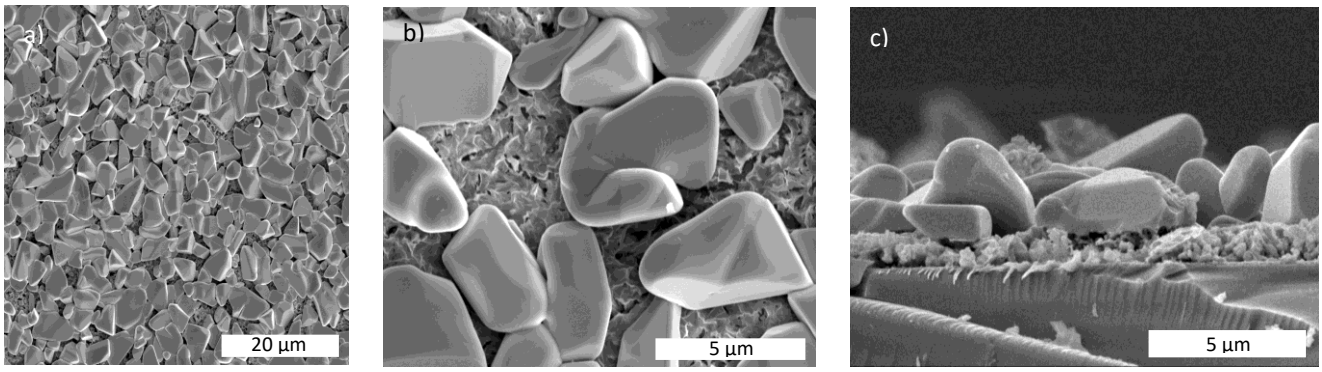

Figure S16. a) SEM top-view at low magnification, b) SEM top-view at high magnification c) SEM cross-sectional view of $AgInSe_2$ film selenized at 515 ^oC on shims with Alumina back contact. There is layer of fine AgInSe2 grains at the bottom of the film.

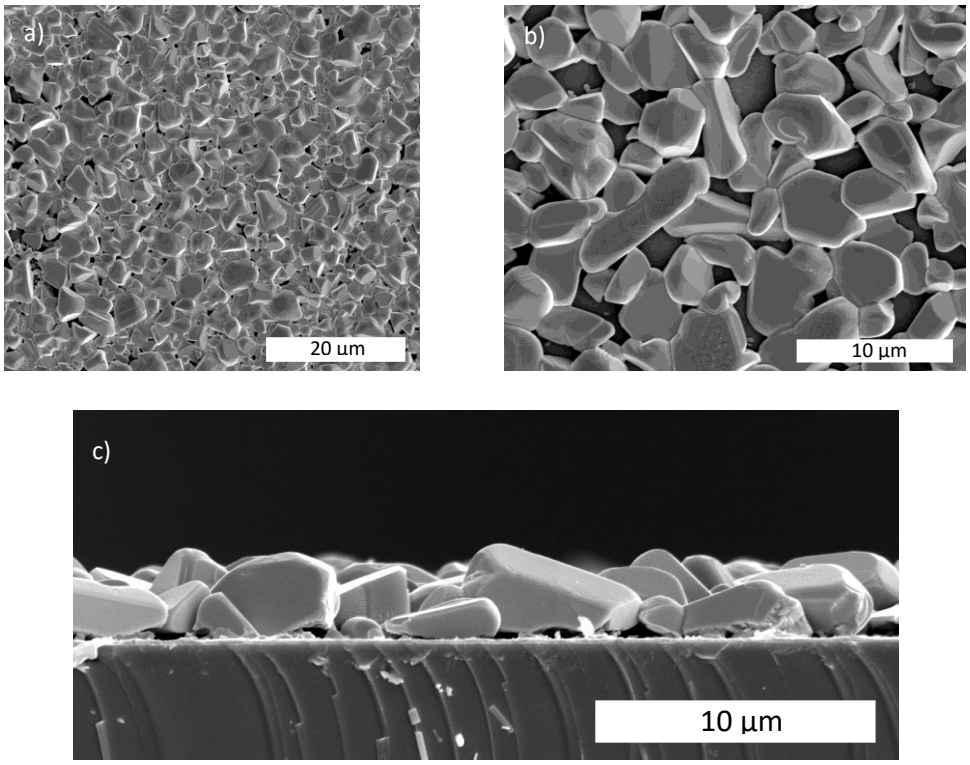

Figure S17. a) SEM top-view at low magnification, b) SEM top-view at high magnification c) SEM cross-sectional view of $AgInSe_2$ film selenized at 600 ^{o}C on shims with Alumina back contact.

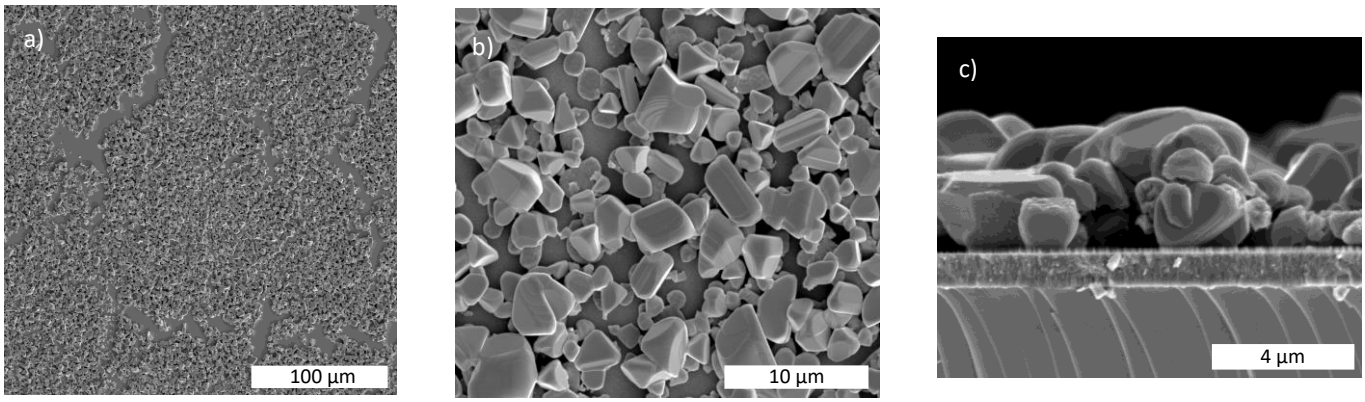

Figure S18. a) SEM top-view at low magnification, b) SEM top-view at high magnification c) SEM cross-sectional view of $AgInSe_2$ film selenized at 600 ^oC on shims with Mo back contact.

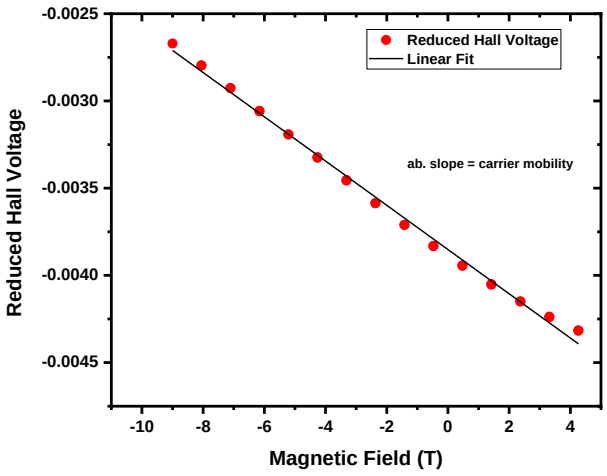

Figure S19. Plot showing the variation of the reduced Hall voltage with the magnetic field. The slope of the curve represents the carrier mobility.